

# FEA-Based Calculation of Performances of IPM Machines with Five Topologies for Hybrid-Electric Vehicle Traction

Aimeng Wang, Dejun Ma, and Hui Wang

**Abstract**—The paper presents a detailed calculation of characteristic of five different topology permanent magnet machines for high performance traction including hybrid -electric vehicles using finite element analysis (FEA) method. These machines include V-shape single layer interior PM, W-shape single-layer interior PM, Segment interior PM and surface PM on the rotor and with distributed winding on the stator. The performance characteristics which include the back-emf voltage and its harmonic, magnet mass, iron loss and ripple torque are compared and analyzed. One of a 7.5kW IPM prototype was tested and verified finite-element analysis results. The aim of the paper is given some guidance and reference for machine designer which are interested in IPM machine selection for high performance traction application.

**Keywords**—Interior permanent magnet machine, finite-element analysis (FEA), five topologies, electric vehicle.

## I. INTRODUCTION

THE basic requirements of electric machine for traction application include high torque density, high power density and wide speed range for a constant power operation and high efficiency. Interior permanent magnetic (IPM) machine can be optimized design to offer above advantages and has emerged as popular choices for high performance traction including hybrid -electric vehicles, as in [1]-[3]. It has been reported the several novel permanent magnet rotor structure influence its performance and it can be extended the constant-power speed range in IPM machine by optimizing design in [4]-[7]. Reference [4] has summarized that the wide speed range for constant power can be improved by adding the layer of interior permanent magnetic (PM) rotor barrier.

The paper optimized a 7.5 kW PM machine in five different topology including V-shape single layer interior PM, W-shape interior PM, Segmented interior PM and surface PM on the rotor and with distributed winding on the stator. Detailed comparisons of the performance characteristics are presented. Finally, we used the limited facility to test the performance of one kind of IPM machine and get a good agreement with finite- element analysis results.

## II. FIVE TOPOLOGY IPM MACHINE DESIGN

A 7.5 kW IPM machine with five kinds of permanent magnet rotor were designed as shown in Fig. 1. The five kinds

of topology machine with same stator consists of double-layer distributed windings and were optimized for achieving wide range of constant power operation by means of flux-weakening. Fig. 1 (a) is surface PM (SPM) synchronous machine which has poor flux-weakening capability because of its  $L_d=L_q$ . Fig. 1 (b)-(e) are cross-sections of interior PM synchronous machines, which have generally been considered to be a good candidates for achieving wide speed range of constant power operation, to satisfy performance requirements of hybrid-electric vehicles application [7], [8]. Fig. 1 (e) is a proposed a novel PM rotor structure who has an excellent flux-weakening performance. The major design parameters are shown in Table I.

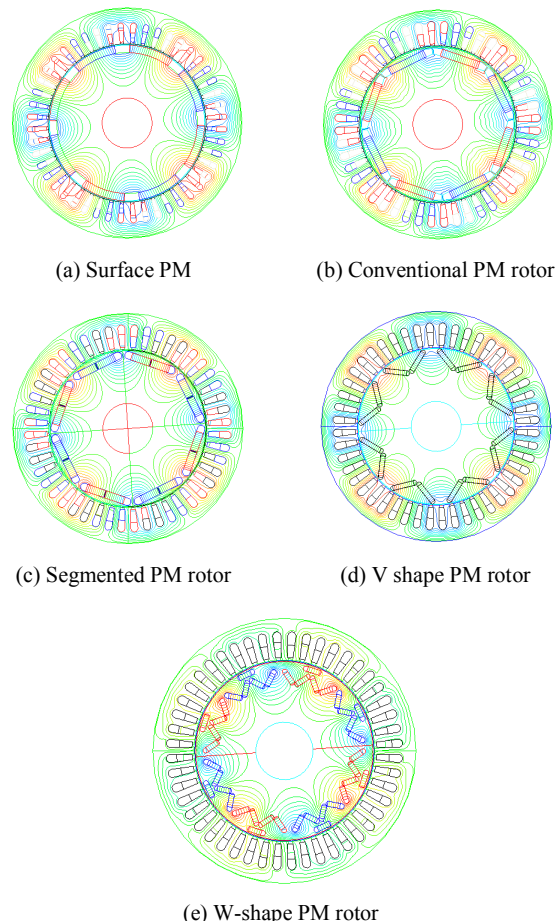


Fig. 1 Cross-sections of 7.5 kW PM flux distributions of the five machines design at no-load condition

Aimeng Wang, Dejun Ma, and Hui Wang are with State Key Laboratory of Alternate Electrical Power System with Renewable Energy Sources, North China Electric Power University, Baoding, China (e-mail: Aimeng@ncepu.edu.cn, mdjhm@126.com, Hui.wang@ncepubd.edu.cn).

TABLE I  
PARAMETERS OF 7.5KW IPM MACHINE

Parameters	Value
Power	7.5kW
Rated voltage	115V
Pole pairs	4
Rated speed	3200rpm
Slots of stator	48
Out diameter of stator	φ175mm
Inner diameter of stator	φ120mm
Length of core	75mm
Inner diameter of rotor	φ38mm
Air gap	0.5mm
Thickness of PM	3.3~5.5 mm

### III. PERFORMANCE COMPARISONS FOR THE FIVE TOPOLOGY PM MACHINE

#### A. Parameters Calculation

The impact of magnetic saturation on inductance is that the value of inductance is not a constant, which varied with current changing. The d-and q-axis inductances are calculated as follows in [9]:

$$L_d = \frac{\lambda_d - \lambda_{PM}}{I_d} /_{i_q=0} \quad (1)$$

$$L_q = \frac{\lambda_q}{I_q} /_{i_d=0} \quad (2)$$

$\lambda_{PM}$  is magnet flux-linkage generated by PM.

The FEA- calculated d-and q-axis inductance for comparisons are shown in Fig. 2. It is well known that the condition for optimal flux weakening in IPM machine occurs when the machine characteristic current equals the rated current, that is

$$I_{ch} \equiv \frac{\lambda_{pm}}{L_d} \quad (3)$$

From Fig. 2 can be seen that the inductance values of SPM machine are typically low, so its characteristic current tend to be significantly higher than rated current, which limits on the SPM machine's achievable constant-power speed range (CPSR) [10]. While in interior PM machine including conventional, Segmented PM rotor structure, both d- axis inductances and the q- axis inductances are larger than SPM machine, the W-shape PM rotor one has the largest inductances among them.

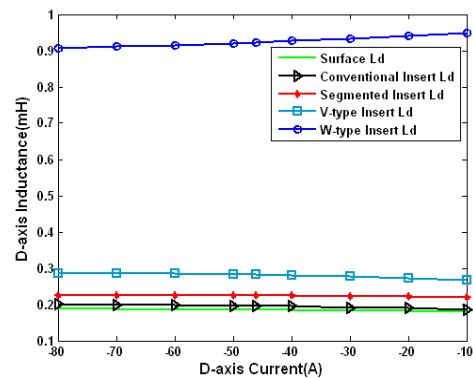
#### B. Magnet Length and Mass

Table II summarized the magnet mass among five topology and the comparisons are shown in Fig. 3. Since the d-axis inductances is smaller than the q-axis inductances in interior PM machine, a reluctance torque exists and results for less mass to produce same output torque comparing with SPM machine. Fig. 3 shows V-shaped and W-shaped IPM designs

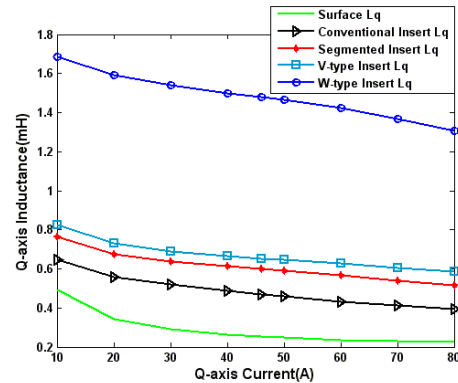
have lower magnet mass compared to the other three PM designs.

#### C. Back-EMF and Ripple Torque Comparison

Pulsating torque is harmonic torque which is caused by the interaction between induced EMF harmonic and the stator current harmonic. In order to reduce the ripple torque, the harmonic are minimum as much as possible in the process of motor design, while induced EMF harmonic is related with the spatial distribution and winding design of excitation magnetic field produced by magnets. The No-load back-EMF and its harmonic analysis of the five comparisons are given in Table III. It were shown that the total harmonic distortion (THD) of segmented PM rotor and W-shape PM rotor are lower than that of the conventional PM motor, However, the amount of harmonic of V-shape PM rotor is relatively large.



(a) D-axis inductance



(b) Q-axis inductance

Fig. 2 Comparisons of inductance of five topology machine

TABLE II  
MAGNET MASS AND DIMENSION

Topology	Magnet	Thickness (mm)	Mass (g)	Length/per pole (mm)
Surface PM		5.5	826.14	33.3794
Conventional IPM		5.5	742.4	30
Segmented IPM		5.5	724.4	29.2531
V-shape IPM		3.5	513.44	32.6
W-shape IPM		3.3	632.56	42.6

PM material: NdFe35, Br: 1.23T, Hc: 978.803kA/m, density: 7.5g/cm<sup>3</sup>

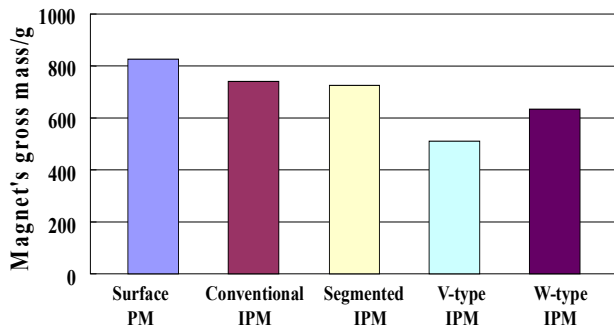


Fig. 3 Comparisons of magnet's gross mass of five topology machine

The ripple torque calculation is defined as:

$$T_{Ripp.} = (T_{Max} - T_{Min}) / T_{Aveg.} \quad (4)$$

The output average torque vs. electric degree for conventional PM machine is shown in Fig. 4. Using (4), the comparison of the five topology machines' ripple torque at the different current value is shown in Fig. 5. Inspection of it indicates that the ripple torque of segmented PM rotor and W-shape PM rotor are lower than that of conventional PM motor. In contrast, the ripple torque of the surface PM and V-shape PM rotor are relatively large at the condition of rated current. This situation will change with the current increase or decrease. Normally the harmonic will influence the scale of the ripple torque, the greater the amount of harmonic the greater the ripple torque.

#### D. Flux-Weakening Performance

The flux weakening index (FWI) defined as the ratio of the rated current to the machine characteristic current, expressed as following:

$$\rho = \frac{L_d I_r}{\lambda_{PM}} \quad (5)$$

$I_r$  is rated current, when the FWI value  $\rho$  is close to 1, its speeds can be up to infinite. The Flux-weakening capability can be improved significantly by optimizing the design of the IPM machine. The comparison of FWI value of five topologies is shown in Table IV. From the Table IV, we can see that the FWI of W-shape PM is the highest and close to 1, followed by V-shape PM, segmented PM, conventional PM and the surface PM machine five topology machines are operated with voltage constraint. The torque vs. speed as well as power vs. speed performance at the rated current are plotted in Figs. 6, 7.

Inspection of Figs. 6, 7 indicates that w-shape has wider constant power speed range and can exhibits more torque than other three kinds of IPM machine at the constant torque range as well. While V-shape machine has moderate flux-weakening performance even it has lowest magnet mass than other four.

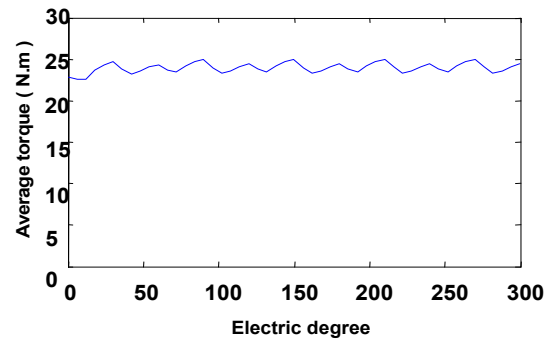


Fig. 4 Averaged torque of conventional IPM machine vs. electric degree

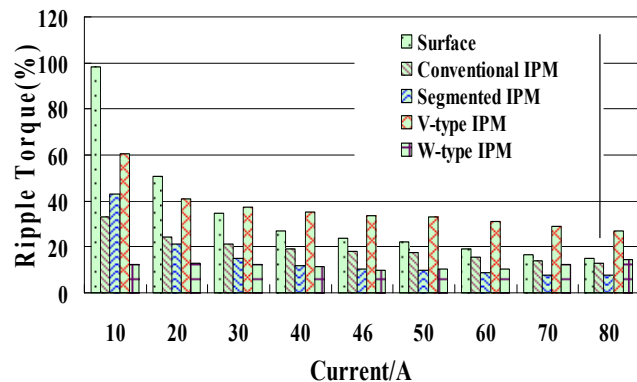


Fig. 5 Comparisons of ripple torque of the five machines

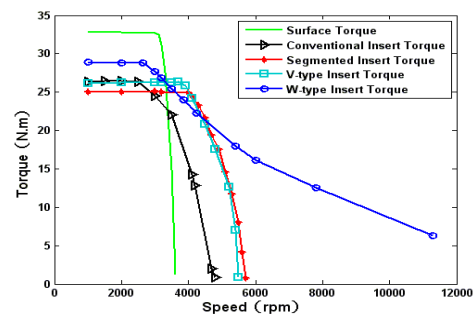


Fig. 6 Comparisons of torque-speed characteristic of the five machines

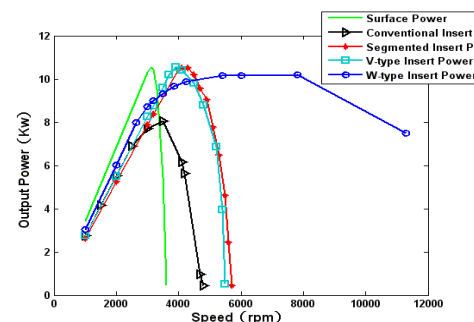


Fig. 7 Comparisons of power-speed characteristic of the five machines

TABLE III  
THE BACK-EMF AND ITS HARMONIC ANALYSIS

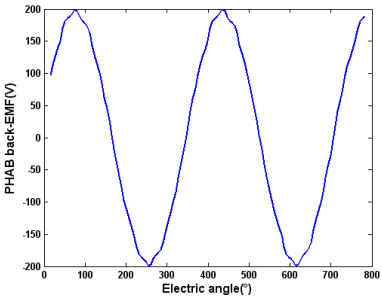
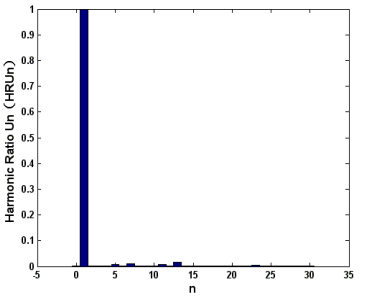
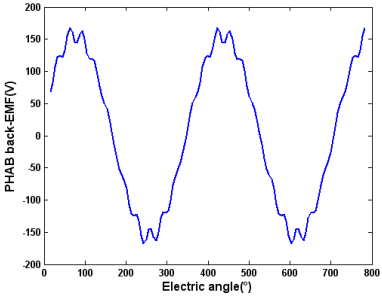
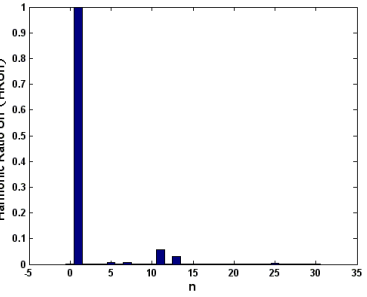
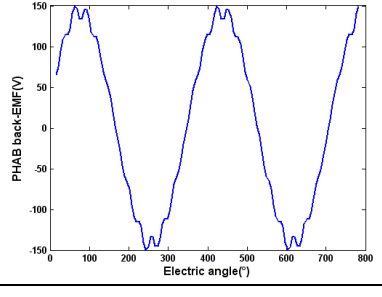
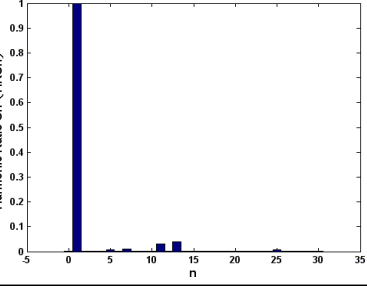
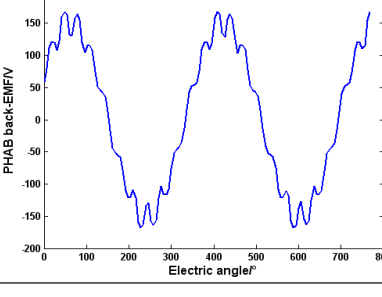
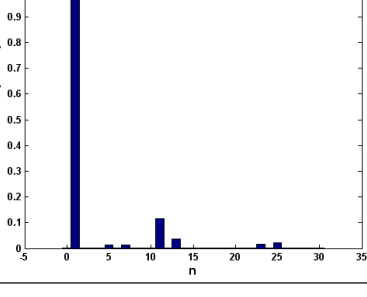
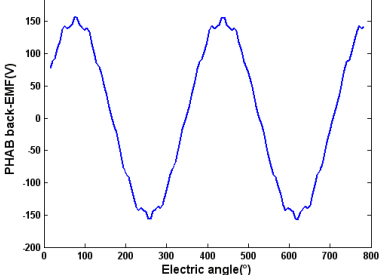
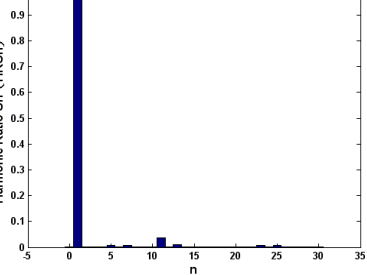
Rotor	Back-emf Wave Ph-AB	Harmonics	ThD(%)
Surface			2.1%
Conventional IPM			6.7%
Segmented IPM			5.2%
V-type IPM			12.5%
W-type IPM			4.1%

TABLE IV  
THE FWI VALUE OF FIVE TOPOLOGY MACHINE

Topology	FWI
SPM	0.102205
Conventional PM	0.135646
Segmented PM	0.170014
V shape PM	0.210179
W shape PM	0.628795

#### IV. PARAMETER TEST

We used the limited facility to test the performance of a 7.5 kW IPM prototype with conventional magnet IPM machine. The test equipments are shown in Fig. 8.

Using Static inductance measurement method [11], the connection diagram is shown in Fig. 9.

Excite machine with low voltage AC from an auto-transformer and slowly rotate rotor, when rotor is aligned with  $d$ -axis: currents  $I_B$  and  $I_C$  are equal and are large in value, Then rotate rotor to find  $q$ -axis: currents  $I_B$  and  $I_C$  are equal and are small in value record rms terminal voltage  $V$  and current  $I$ .

The flux-linkage found by integrating the voltage minus resistance drop, as following:

$$\lambda(t) = \int v(t) - Ri(t) dt \quad (6)$$

The phase inductance should be:

$$L(t) = \frac{2}{3} \frac{\lambda(t)}{i(t)} \quad (7)$$

The  $d$ - and  $q$ -axis inductance versus current are shown in Fig. 11. The inductance of  $d$ - $q$  axis in Fig. 11 is identical with the FEA results. At the condition of rate speed and open circuit, the measurement of the output voltage is shown as Fig. 12. The iron loss versus speed test data is shown in Fig. 13.

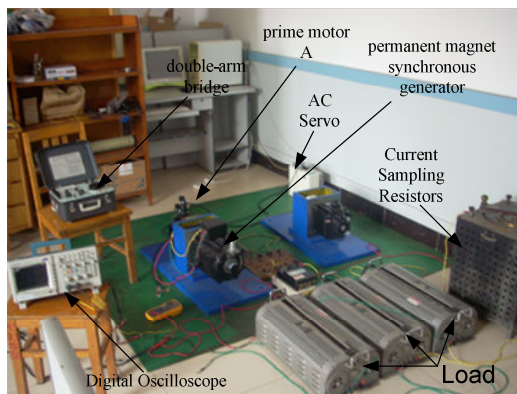


Fig. 8 A view of the test equipment

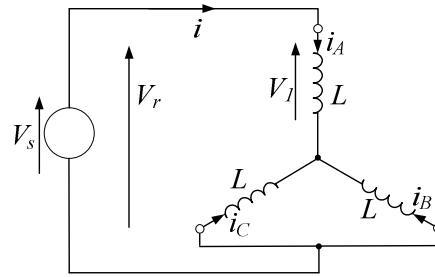


Fig. 9 Three-phase connection used when measuring inductance using a single-phase excitation

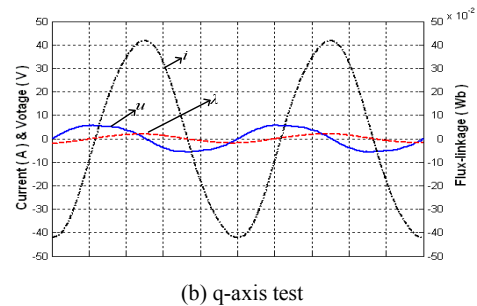
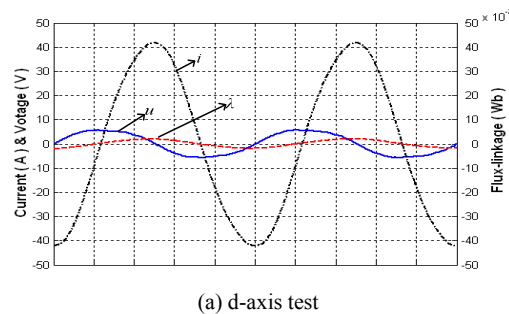
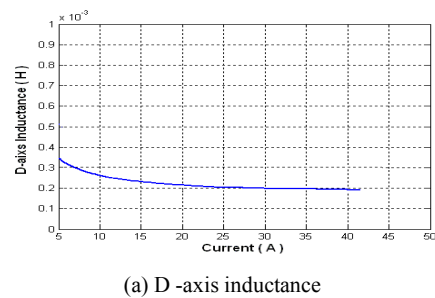
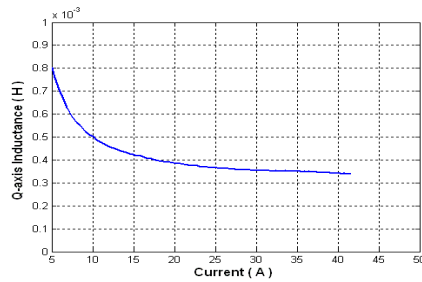


Fig. 10 Two cycles of the measured voltage and current waveforms and the calculated flux-linkage waveform





(b) Q -axis inductance

Fig. 11 Measure d-axis and q-axis inductance with conventional magnet machine

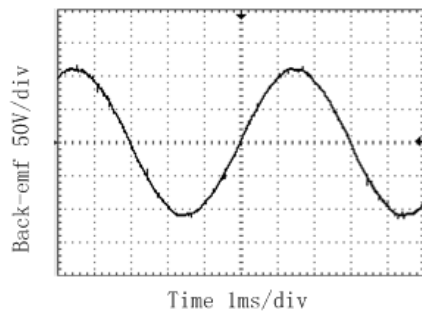


Fig. 12 Back-emf at 3000rpm

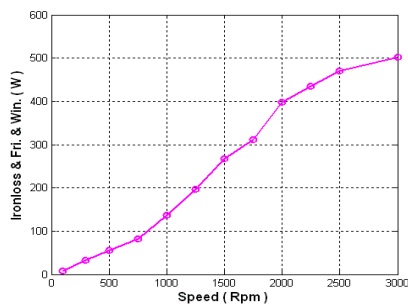


Fig. 13 Loss vs. speed

## V. CONCLUSIONS

This paper compares the performance of the five topology PM machine for electric vehicle traction application, obtaining the following conclusions:

- The waveforms of Back-EMF can optimized to be as sinusoidal by shaping and changing the position of PM rotor.
- V-shape PM rotor has less magnet mass to produce the same output torque among 5 kinds of machine.
- W-shape PM has a largest d- and q-axis inductance, followed by V-shape PM, the surface PM has the lowest.
- Segment PM motor has a wider range of constant power operation than that of conventional PM motor since its capacity of flux-weakening is decrease because of having the magnetic flux flow path between the two permanent magnets.

- W-shape PM machine has the best flux-weakening performance and has wider constant-power operating range and can meet the electric vehicles requirements.

By optimizing the shape and position of permanent magnet, the performance of permanent magnet synchronous motor has been further improved and more suitable for hybrid electric traction application.

## ACKNOWLEDGMENT

The authors acknowledge the financial support by the Fundamental Research Funds for the Central Universities of China (13MS76) and the Natural Science Foundation of Hebei Province (E2012502018) of China.

## REFERENCES

- [1] T. M. Jahns, "Flux-weakening regime operation of an interior permanent magnet synchronous motor drive," IEEE Trans. Ind. Appl., vol. 23, pp.681–689, Jul./Aug. 1987
- [2] Wen L. Song, Nesimi Ertugrul, "Field-Weakening Performance of Interior Permanent-Magnet Motors", IEEE Transactions on Industry applications, Vol.38. NO.5, pp.1251-1258, 2002
- [3] Thomas M. Jahns, Seok-Hee Han, Ayman M. EL-Refaie, Jei-Hoon Baek. "Design and Experimental Verification of a 50 Kw Interior Permanent Magnet Synchronous Machine". IEEE Trans. on Ind. IAS. Page(s):1941-1948, Oct. 2006
- [4] W. L. Soong, S. Han, and T. M. Jahns. Design of Interior PM Machines for Field-Weakening Applications [J]. ICEMS, Seoul, Korea 2007:654-664.
- [5] Y. Honda, T. Nakamura, T. Higaki, and Y. Takeda. Motor Design Considerations and Test Results of an Interior Permanent Magnet Synchronous Motor for Electric Vehicles [J]. IEEE IAS Annual Meeting, 1997,1: 75-82.
- [6] F. Rahman, R. Dutta. A New Rotor design of Interior Permanent Magnet machine suitable for wide speed range [J]. IEEE Trans. on Ind. IECON, Nov. 2003, 1:699 -704.
- [7] Wang Aimeng, Li Heming, Lu Weifui "Influence of skew and Segment magnet rotor on Interior Permanent Magnet Machine Performance and Torque Ripple for Electric Traction", IEMDC2009, pp358-363 .
- [8] W. Soong, T. J. E. Miller, "Field Weakening Performance of Brushless Synchronous AC Motor Drives", IEE Proceedings-Electric Power Applications, vol. 141, no. 6, November 1994, pp. 331-340.
- [9] Aimeng Wang, T. M. Jahns "Accuracy Investigation of Closed-Form Predictions for the Operating Envelope Performance Characteristics of Interior PM Synchronous Machines" Proceeding of the IEEE-IEMDC'07, Oct. 8~11, Seoul, Korea, pp. 486-489
- [10] A. M. EL-Refaie and T. M. Jahns, "Optimal flux weakening in surface PM machines using concentrated windings," IEEE Trans. Ind. Appl., vol. 41, no. 3, pp. 790–800, May/Jun. 2005.
- [11] W. L. Soong "Power Engineering Briefing Note Series for Inductance Measurements for Synchronous Machines" 8 May 2008.

**Aimeng Wang** was born in 1963. She is an Associate Professor at North China Electric Power University, Baoding, China. Her research area includes the permanent magnet motor design and its drive control system.

**Dejun Ma** was born in 1986. He is a Master graduate student at North China Electric Power University, Baoding, China. His research area includes permanent magnet motor design.

**Hui Wang** was born in 1988. He is a Master graduate student at North China Electric Power University, Baoding, China. His research area includes the study of the permanent magnet motor.